

Recent results from LHCb

Justine Serrano*

On behalf of the LHCb Collaboration

CPPM, Aix-Marseille Université, CNRS/IN2P3, Marseille, France

E-mail: serrano@cppm.in2p3.fr

Recent results from the LHCb experiment are presented. Most of them are based on the whole statistic accumulated during the year 2011. After a short introduction, selected topics on rare B decays, CP violation, and spectroscopy are presented. A brief discussion of the LHCb Upgrade is also given.

*The 30 International Symposium on Lattice Field Theory - Lattice 2012,
June 24-29, 2012
Cairns, Australia*

*Speaker.

1. Introduction

LHCb is a forward spectrometer optimised for heavy flavour physics at the LHC. The precise vertexing, very efficient particle identification, low trigger threshold, and large boost of b and c hadrons allow to study a large number of heavy flavour hadron decays. The LHCb programme is focused on searching for physics beyond the Standard Model (SM), referred to as “New Physics” (NP), with an approach complementary to that used by the ATLAS and CMS experiments. While the high- p_T experiments search for on-shell production of new particles, LHCb can look for their effects in processes that are precisely predicted in the SM. In order to perform precision physics analyses and due to the limited hardware trigger rate at 1MHz, LHCb takes data in a low pile-up environment at a constant luminosity of $\mathcal{L}_{\text{inst}} = 4.10^{32} / \text{cm}^2 / \text{s}$.

During 2011, the LHC machine and the LHCb detector had excellent performances, allowing LHCb to accumulate 1.0 fb^{-1} of $\sqrt{s} = 7 \text{ TeV}$ pp collisions available for physics analysis. Thanks to the large $b\bar{b}$ production cross-section, $\sigma(pp \rightarrow b\bar{b}X) = (89.6 \pm 6.4 \pm 15.5) \mu\text{b}$ in the LHCb acceptance [1], and a $c\bar{c}$ production cross-section about 20 times larger [2], these data provide unprecedented samples of heavy flavoured hadrons.

In the following, a review of recent LHCb results will be presented, focusing on selected topic from rare B decays (Sec. 2), CP violation, and mixing (Sec. 3), and spectroscopy (Sec.4). Finally a discussion of the LHCb Upgrade will also be carried out (Sec. 5).

2. Rare B decays

2.1 Introduction

In the following, we will concentrate on flavour changing neutral current (FCNC) processes that are mediated by electroweak box or penguin diagrams in the SM. These processes provide good observables to look for NP, as new particles at the TeV scale can enter the loop and modify branching fractions or angular distributions of the daughter particles in these decays. More precisely, we will focus on rare B decays involving leptons or photons in the final states, though there are also interesting results on rare decays in the charm sector and rare hadronic B decays.

Contributions from physics beyond the SM to the observables in rare radiative, semi-leptonic, and leptonic B decays can be described by the modification of Wilson coefficients of local operators in an effective Hamiltonian of the form

$$\mathcal{H}_{\text{eff}} = -\frac{4G_F}{\sqrt{2}} V_{tb} V_{tq}^* \frac{e^2}{16\pi^2} \sum_i (C_i O_i + C'_i O'_i) + \text{h.c.}, \quad (2.1)$$

where $q = d, s$. In many models, the operators that are most sensitive to new physics (NP) are a subset of

$$\begin{aligned} O_7^{(\prime)} &= \frac{m_b}{e} (\bar{q} \sigma_{\mu\nu} P_{R(L)} b) F^{\mu\nu}, & O_8^{(\prime)} &= \frac{gm_b}{e^2} (\bar{q} \sigma_{\mu\nu} T^a P_{R(L)} b) G^{\mu\nu a}, \\ O_9^{(\prime)} &= (\bar{q} \gamma_\mu P_{L(R)} b) (\bar{\ell} \gamma^\mu \ell), & O_{10}^{(\prime)} &= (\bar{q} \gamma_\mu P_{L(R)} b) (\bar{\ell} \gamma^\mu \gamma_5 \ell), \\ O_S^{(\prime)} &= \frac{m_b}{m_{B_q}} (\bar{q} P_{R(L)} b) (\bar{\ell} \ell), & O_P^{(\prime)} &= \frac{m_b}{m_{B_q}} (\bar{q} P_{R(L)} b) (\bar{\ell} \gamma_5 \ell), \end{aligned} \quad (2.2)$$

which are customarily denoted as magnetic ($O_7^{(\prime)}$), chromomagnetic ($O_8^{(\prime)}$), semi-leptonic ($O_9^{(\prime)}$ and $O_{10}^{(\prime)}$), pseudoscalar ($O_P^{(\prime)}$) and scalar ($O_S^{(\prime)}$) operators.¹ While the radiative $b \rightarrow q\gamma$ decays are sensitive only to the magnetic and chromomagnetic operators, semi-leptonic $b \rightarrow q\ell^+\ell^-$ decays are, in principle, sensitive to all these operators.²

Each rare B decay depends on different operators and Wilson coefficients. It is therefore important to combine the informations coming from different analyses to improve the constraints on the Wilson coefficients.

2.2 $B_s^0 \rightarrow \mu^+\mu^-$ and $B^0 \rightarrow \mu^+\mu^-$

The branching fraction of $B_{s(d)}^0 \rightarrow \mu^+\mu^-$ can be written as

$$\begin{aligned} \mathcal{B}(B_q^0 \rightarrow \mu^+\mu^-) &= \frac{G_F^2 \alpha^2}{64\pi^3} f_{B_q}^2 \tau_{B_q} m_{B_q} |V_{tb}V_{tq}^*|^2 \sqrt{1 - \frac{4m_\mu^2}{m_{B_q}^2}} \\ &\times \left\{ \left(1 - \frac{4m_\mu^2}{m_{B_q}^2}\right) |C_S - C_S'|^2 + \left| (C_P - C_P') + 2\frac{m_\mu}{m_{B_q}} (C_{10} - C_{10}') \right|^2 \right\}, \end{aligned} \quad (2.3)$$

where $q = s, d$.

Within the SM, C_S and C_P are negligibly small and the dominant contribution of C_{10} is helicity suppressed.

The SM predictions for these decays are very precise. Up to now, LHC experiments published results comparing to the values given by [3]:

$$\mathcal{B}(B_s^0 \rightarrow \mu^+\mu^-)_{\text{SM}} = (3.2 \pm 0.2) \times 10^{-9}, \quad \mathcal{B}(B^0 \rightarrow \mu^+\mu^-)_{\text{SM}} = (1.1 \pm 0.1) \times 10^{-10}. \quad (2.4)$$

It should be noted that these predictions use experimental determination of Δm_s in order to have a reduced uncertainty on the value of the B_s^0 decay constant, f_{B_s} . With the recent significant improvement of lattice calculations of f_{B_s} , this approach is being abandoned. As example, a new prediction based on the average of f_{B_s} values from Ref. [4], has been done by [5]:

$$\mathcal{B}(B_s^0 \rightarrow \mu^+\mu^-)_{\text{SM}} = (3.1 \pm 0.2) \times 10^{-9}, \quad \mathcal{B}(B^0 \rightarrow \mu^+\mu^-)_{\text{SM}} = (1.0 \pm 0.1) \times 10^{-10}, \quad (2.5)$$

which is in very good agreement with 2.4.

One important point to keep in mind is that when comparing to the experimental measurement, which is time integrated (TA), the theoretical values of the branching fraction (TH), computed at $t = 0$, has to be corrected to take into account the sizable width difference between the heavy and light B_s^0 meson [6, 7]. In general,

$$\mathcal{B}(B_s^0 \rightarrow \mu^+\mu^-)_{\text{TH}} = [(1 - y_s^2)/(1 + \mathcal{A}_{\Delta\Gamma} y_s)] \times \mathcal{B}(B_s^0 \rightarrow \mu^+\mu^-)_{\text{TA}} \quad (2.6)$$

where $\mathcal{A}_{\Delta\Gamma} = +1$ in the SM and $y_s = 0.088 \pm 0.014$ [8]. Thus the experimental measurements have to be compared to the following SM prediction for the time-averaged branching fraction:

¹In principle there are also tensor operators, $O_{T(5)} = (\bar{q}\sigma_{\mu\nu}b)(\bar{\ell}\sigma^{\mu\nu}(\gamma_5)\ell)$, which are relevant for some observables.

²In radiative and semi-leptonic decays, the chromomagnetic operator O_8 enters at higher order in α_s .

$$\mathcal{B}(B_s^0 \rightarrow \mu^+ \mu^-)_{\text{SM,TA}} = \mathcal{B}(B_s^0 \rightarrow \mu^+ \mu^-)_{\text{SM,TH}} / (1 - y_s) = (3.5 \pm 0.2) \times 10^{-9}. \quad (2.7)$$

New Physics models, especially those with an extended Higgs sector, can significantly enhance the $B_{s(d)}^0 \rightarrow \mu^+ \mu^-$ branching fraction even in the presence of other existing constraints. In particular, the decay $B_s^0 \rightarrow \mu^+ \mu^-$ is very sensitive to the presence of SUSY particles. At large $\tan\beta$, the SUSY contribution to this process is dominated by the exchange of neutral Higgs bosons, and both C_S and C_P can receive large contributions from scalar exchange.

The search for $B_s^0 \rightarrow \mu^+ \mu^-$ and $B^0 \rightarrow \mu^+ \mu^-$ is performed at LHCb using 1.0 fb^{-1} of data. The events selected by the trigger and passing a first selection step are given a probability to be signal or background in a two-dimensional space formed by two independent likelihoods: the di-muon invariant mass and the output of a multivariate classifier. This classifier is a boosted decision tree (BDT) built with geometrical and kinematic variables characteristic to these decays. It is optimized on Monte Carlo simulated events (MC), and built to be uniformly distributed between 0 and 1 for the signal and peaked at 0 for the combinatorial background. The calibrations of the invariant mass and the BDT likelihood are obtained from data using control samples. In order to avoid unconscious biases, the data in the signal region corresponding to a $\pm 60 \text{ MeV}/c^2$ window around the nominal B_s^0 and B^0 mass have been blinded until the completion of the analysis.

The number of expected signal events is obtained by normalizing to channels of known branching ratios according to:

$$\mathcal{B} = \mathcal{B}_{\text{norm}} \times \frac{\epsilon_{\text{norm}}}{\epsilon_{\text{sig}}} \times \frac{f_{\text{norm}}}{f_{d(s)}} \times \frac{N_{B_{(s)}^0 \rightarrow \mu^+ \mu^-}}{N_{\text{norm}}}, \quad (2.8)$$

where $\mathcal{B}_{\text{norm}}$ is the branching fraction of the normalization channel, $\frac{\epsilon_{\text{norm}}}{\epsilon_{\text{sig}}}$ the ratio of efficiencies, $\frac{f_{\text{norm}}}{f_{d(s)}}$ the ratio of hadronization fractions, and $\frac{N_{B_{(s)}^0 \rightarrow \mu^+ \mu^-}}{N_{\text{norm}}}$ the ratio of observed signal and normalization mode candidates. The use of a relative normalization avoid to have to know the luminosity and production cross section. Moreover, ratio of efficiencies are better determined than absolute one. The normalization channels we use are $B^+ \rightarrow J/\psi K^+$, $B_s^0 \rightarrow J/\psi \phi$, and $B^0 \rightarrow K^+ \pi^-$.

The ratio of hadronisation fractions $\frac{f_{\text{norm}}}{f_{d(s)}}$ is determined by LHCb using hadronic [9] and semileptonic [10] decays. We use the combination of these two independent measurements that has a 8% precision [11]. It can be noted that the dominant systematic error in the hadronic measurement is due to the form factor ratio

$$\mathcal{N}_F = \left(\frac{f_0^{(s)}(M_\pi^2)}{f_0^{(d)}(M_K^2)} \right)^2, \quad (2.9)$$

where $f_0^{(s,d)}$ are the form factors of the semileptonic decays $B_s \rightarrow D_s$, $B \rightarrow D$. The LHCb publication uses a value of \mathcal{N}_F determined from QCD sum-rules: $\mathcal{N}_F = 1.24 \pm 0.08$. A new computation of this ratio has been done recently on the lattice by the Fermilab Lattice and MILC collaboration [12]. They find $\mathcal{N}_F = 1.094 \pm 0.088 \pm 0.030$, which has a slightly larger error than the sum-rules determination but can be improved adding MC statistics.

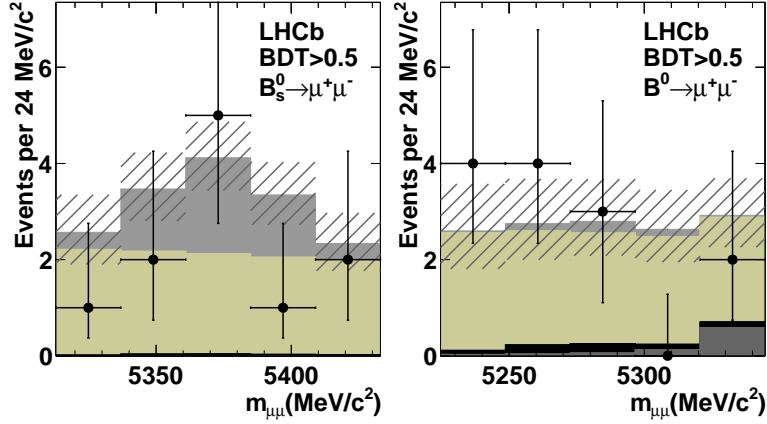


Figure 1: Distribution of selected candidates (black points) in the (left) $B_s^0 \rightarrow \mu^+ \mu^-$ and (right) $B^0 \rightarrow \mu^+ \mu^-$ mass window for $\text{BDT} > 0.5$, and expectations for, from the top, $B_s^0 \rightarrow \mu^+ \mu^-$ SM signal (gray), combinatorial background (light gray), $B_{(s)}^0 \rightarrow h^+ h^-$ background (black), and cross-feed of the two modes (dark gray) [13]. The hatched area depicts the uncertainty on the sum of the expected contributions.

The distributions of the candidates found in 1.0 fb^{-1} of data is shown in Fig. 1 for B_s^0 and B^0 decays in the high BDT region, where the sensitivity is maximised [13].

No excess of events is observed with respect to the expected background and signal from SM. The limit is extracted using a modified frequentist approach, taking into account the crossfeed between the two decay channels. A limit at 95% confidence level of $7.2 (1.1) \times 10^{-9}$ is expected for the B_s^0 (B^0) channel. The observed limits are :

$$\mathcal{B}(B_s^0 \rightarrow \mu^+ \mu^-)_{LHCb} < 4.5 \times 10^{-9}, \mathcal{B}(B^0 \rightarrow \mu^+ \mu^-)_{LHCb} < 1.0 \times 10^{-9}. \quad (2.10)$$

A 1σ downward fluctuation is seen for the $B_s^0 \rightarrow \mu^+ \mu^-$ channel with respect to the SM prediction.

The results of LHCb, ATLAS, and CMS on data collected in 2010 and 2011 have been combined, giving the best exclusion limits on these decays [14]:

$$\mathcal{B}(B_s^0 \rightarrow \mu^+ \mu^-) < 4.2 \times 10^{-9}, \mathcal{B}(B^0 \rightarrow \mu^+ \mu^-) < 8.1 \times 10^{-10}. \quad (2.11)$$

The exclusion limit on the branching fraction of $B_s^0 \rightarrow \mu^+ \mu^-$ decay only 20% above the SM value provide stringent test of possible extensions of the SM. Figure 2 shows the plane $(m_{1/2}, m_0)$ for large and moderate $\tan\beta$ in the CMSSM where, for comparison, direct search limits from CMS are superimposed. It can be seen that, at large $\tan\beta$, the constraints from flavour observables – in particular $\mathcal{B}(B_s^0 \rightarrow \mu^+ \mu^-)$ – are more constraining than those from direct searches. As soon as one goes down to smaller values of $\tan\beta$, the flavour observables start to lose importance compared to direct searches. On the other hand, $B \rightarrow K^* \mu^+ \mu^-$ related observables, in particular the forward backward asymmetry, lose less sensitivity and could play a complementary role.

The correlation between both decays also allows to discriminate between classes of new physics models, as shown in Fig. 3. A large part of the parameter space of the supersymmetric models, where $\tan\beta$ can be large, is ruled out by the constraints. However, in models where NP enters via the semi-leptonic operators $O_{10}^{(\prime)}$, such as the Standard Model with a sequential fourth

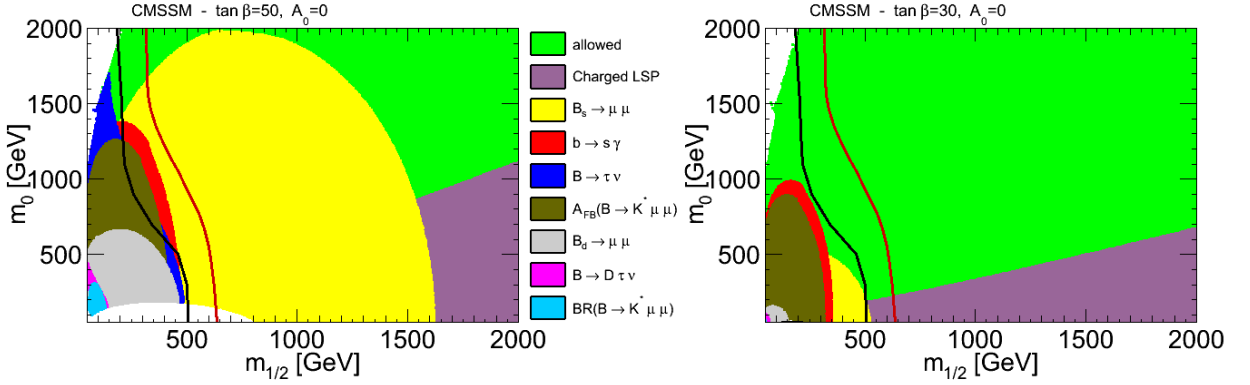


Figure 2: Constraints from flavour observables in CMSSM in the plane $(m_{1/2}, m_0)$ with $A_0 = 0$, for $\tan\beta = 50$ (left) and 30 (right) [15], using SuperIso. The black (red) line corresponds to the CMS exclusion limit with 1.1 (4.4) fb^{-1} of data.

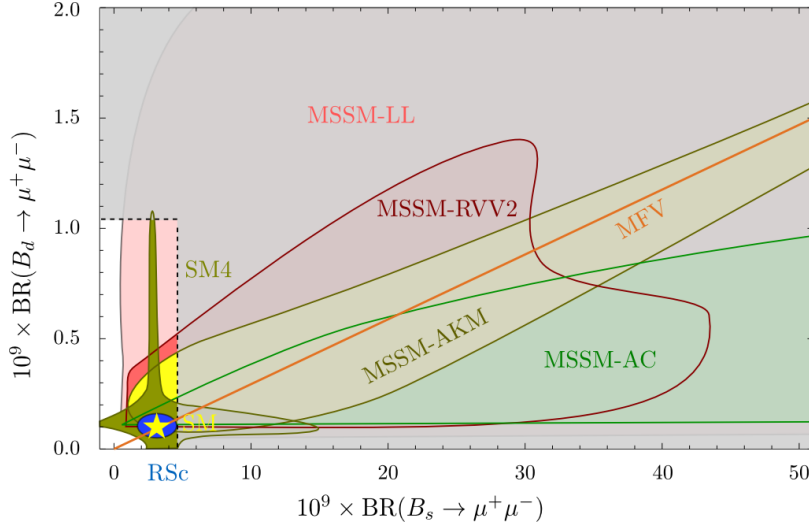


Figure 3: Correlation between $B_s^0 \rightarrow \mu^+ \mu^-$ and $B^0 \rightarrow \mu^+ \mu^-$ in MFV, the SM4 and four SUSY flavour models [16]. The grey area is ruled out experimentally. The SM point is marked by a star.

generation (SM4) or Randall- Sundrum models (RSc) are starting to be probed only now. See Ref. [16] for a detailed discussion of all models shown in Fig. 3.

2.3 Rare semileptonic decays

2.3.1 $B^0 \rightarrow K^* \mu^+ \mu^-$

The $B^0 \rightarrow K^* \mu^+ \mu^-$ decay provide strong constraints on $C_7^{(\prime)}$, $C_9^{(\prime)}$ and $C_{10}^{(\prime)}$ through their angular observables. The differential decay rate depends on four variables: the dilepton invariant mass squared, q^2 , the angle between the muon in the dimuon rest frame and the dimuon in the B^0 rest frame, θ_l , the angle between the kaon in the K^* rest frame and the K^* in the B^0 rest frame θ_K , and the angle between the decay planes of the dimuon and the K^* systems in the B^0 rest frame, ϕ .

The full $B^0 \rightarrow K^{*0} \mu^+ \mu^-$ differential decay distribution is parameterised by six q^2 dependent amplitudes. In the LHCb analysis, a symmetry of the system is exploited and ϕ is transformed to

$\phi \rightarrow \phi + \pi$ when $\phi < 0$. This cancels terms with $\cos\phi$ and $\sin\phi$ dependences and decreases the number of parameters required to describe the signal. This “folding” leads to a reduced expression for the angular distribution:

$$\frac{1}{\Gamma} \frac{d^4\Gamma}{d\cos\theta_\ell d\cos\theta_K d\phi dq^2} = \frac{9}{16\pi} \left[F_L \cos^2\theta_K + \frac{3}{4}(1-F_L)(1-\cos^2\theta_K) - F_L \cos^2\theta_K(2\cos^2\theta_\ell - 1) + \frac{1}{4}(1-F_L)(1-\cos^2\theta_K)(2\cos^2\theta_\ell - 1) + S_3(1-\cos^2\theta_K)(1-\cos^2\theta_\ell)\cos 2\phi + \frac{4}{3}A_{FB}(1-\cos^2\theta_K)\cos\theta_\ell + S_9(1-\cos^2\theta_K)(1-\cos^2\theta_\ell)\sin 2\phi \right].$$

The distribution is parameterised by the four observables: the forward-backward asymmetry A_{FB} , the fraction of longitudinal polarization of the K^* F_L , S_9 , and S_3 . The observable S_3 is related to the asymmetry between the parallel and perpendicular K^* spin amplitude³ and is sensitive to right handed operator ($C_7^{(\prime)}$) at low q^2 .

In 1.0 fb^{-1} of integrated luminosity, LHCb has collected the world’s largest sample of $B^0 \rightarrow K^{*0} \mu^+ \mu^-$ (with $K^{*0} \rightarrow K^+ \pi^-$) decays, with around 900 signal events [17]. To estimate the rate averaged values of F_L , A_{FB} , S_9 , and S_3 , an unbinned maximum likelihood fit is performed to the $K^+ \pi^- \mu^+ \mu^-$ invariant mass and angular distribution of the candidates in six q^2 bins.

The current experimental status of these $B^0 \rightarrow K^{*0} \mu^+ \mu^-$ angular observables at LHCb, the B factories and CDF is shown in Figs. 4. The 68% (statistical) confidence intervals are estimated from the one-dimensional profile-likelihood of F_L , A_{FB} , S_9 and S_3 . The coverage of the intervals has been checked by using an ensemble of simulated experiments. The SM prediction for the angular observables, and the prediction rate-averaged over the q^2 -bin, are also indicated on the figures. No SM prediction is included in the region between the $c\bar{c}$ resonances where the assumptions made in the prediction break down. No theory band is included for S_9 , which is expected to be small, $\mathcal{O}(10^{-3})$ [18], in the SM. The theory predictions are described in Ref. [19] (and references therein).

Whilst A_{FB} is not free from form factor uncertainties at low q^2 , the value of the dilepton invariant mass q_0^2 , for which the differential forward-backward asymmetry A_{FB} vanishes, can be predicted in a clean way. The SM predictions stand in the range $4.0 - 4.3 \text{ GeV}^2/c^4$ [20, 21, 22].

The zero-crossing point in data is extracted using an “unbinned-counting” technique, where the q^2 distribution of forward- and backward-going candidates is extracted separately from data using unbinned maximum-likelihood fits to the $K^+ \pi^- \mu^+ \mu^-$ invariant mass and q^2 distributions. The A_{FB} obtained by this “unbinned counting” method is shown in Fig. 5, for comparison the result of a simple counting method is also shown. The zero-crossing point is measured to be

$$q_0^2 = (4.9_{-1.3}^{+1.1}) \text{ GeV}^2/c^4.$$

³The quantity $S_3 = (1 - F_L)/2 \times A_T^{(2)}$ (in the massless case) allows access to one of the theoretically clean quantities, namely $A_T^{(2)}$.

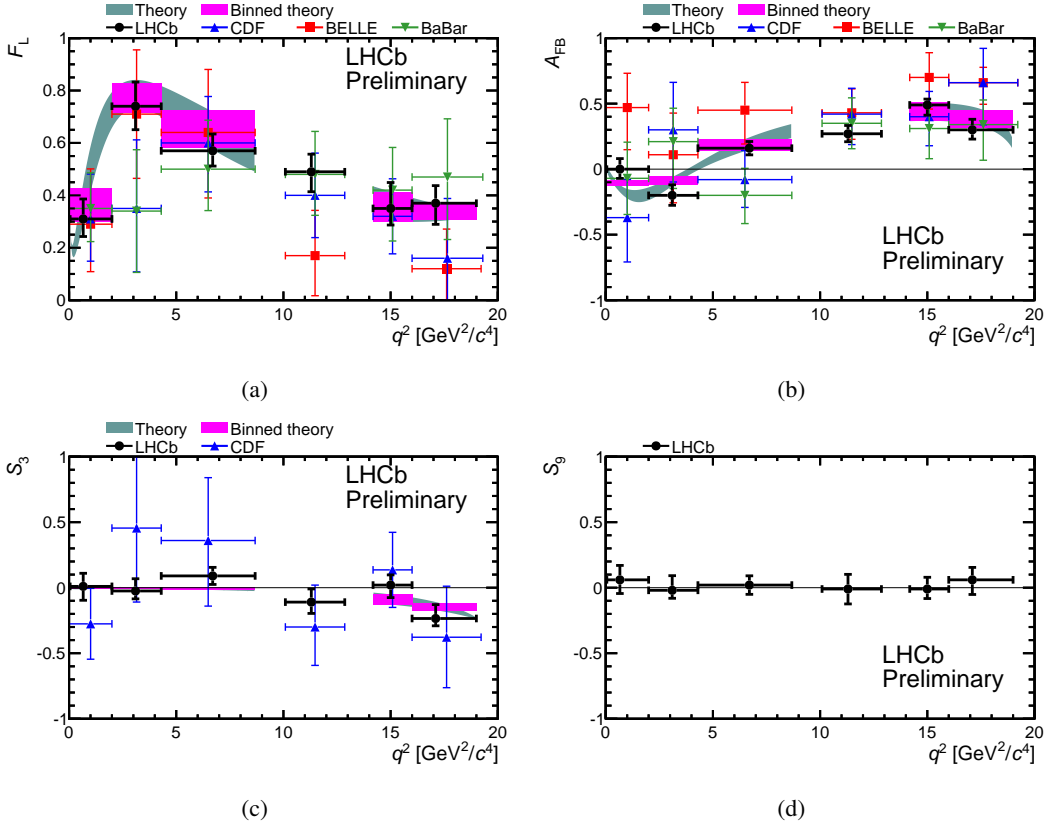


Figure 4: Summary of recent measurements of the angular observables F_L (a), A_{FB} (b), S_3 (c) and S_9 (d) in $B \rightarrow K^* \mu^+ \mu^-$ decays at LHCb, CDF, and the B factories [17]. A description of these observables is provided in the text. The theory predictions at low- and high-dimuon invariant masses are described in Ref. [19] (and references therein).

LHCb has obtained the most precise determination of the angular observables A_{FB} , F_L , S_3 and S_9 , as well as the zero crossing point of the forward-backward asymmetry, in $B^0 \rightarrow K^{*0} \mu^+ \mu^-$ decays. These measurements are consistent with the SM predictions. With the increase of the statistics in the coming years, LHCb will be able to perform a full angular analysis of this decay, exploiting the complete new physics sensitivity of this channel.

2.3.2 Isospin asymmetry in $B \rightarrow K^{(*)} \mu^+ \mu^-$

LHCb has been able to select 60 $B^0 \rightarrow K^0 \mu^+ \mu^-$ decays, reconstructed as $K_S^0 \rightarrow \pi^+ \pi^-$, reporting an observation at 5.7σ for this decay, and 80 $B^+ \rightarrow K^{*+} \mu^+ \mu^-$, reconstructed as $K^{*+} \rightarrow K_S^0 \pi^+$, which are comparable in size to the samples available for these modes in the full data sets of the B factories. The isolation of these rare decay modes enables a measurement of the isospin asymmetry of $B \rightarrow K^{(*)} \mu^+ \mu^-$ decays:

$$A_I = \frac{\mathcal{B}(B^0 \rightarrow K^0 \mu^+ \mu^-) - (\tau_{B^0}/\tau_{B^\pm}) \mathcal{B}(B^\pm \rightarrow K^\pm \mu^+ \mu^-)}{\mathcal{B}(B^0 \rightarrow K^0 \mu^+ \mu^-) + (\tau_{B^0}/\tau_{B^\pm}) \mathcal{B}(B^\pm \rightarrow K^\pm \mu^+ \mu^-)}.$$

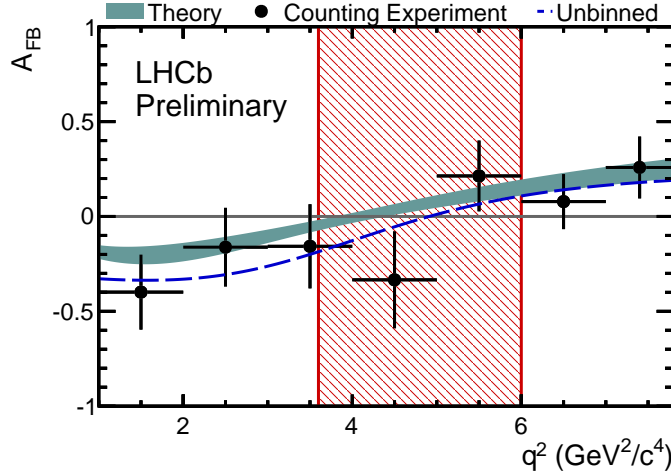


Figure 5: The A_{FB} as a function of q^2 , that comes from the unbinned counting experiment (blue dashed line) overlaid with the theory prediction from Ref. [19]. The data-points are the result of counting forward- and backward-going events in $1 \text{ GeV}^2/c^4$ bins of q^2 [17]. The uncertainty on the data-points is statistical only. The red-hatched region is the 68% confidence interval on the zero-crossing point observed in the data.

At leading order, isospin asymmetries are expected to be zero in the SM. Isospin breaking effects are sub leading Λ/m_b effects, which are difficult to estimate due to unknown power corrections. Nevertheless isospin breaking effects are expected to be small and these observables may be useful in NP searches because they offer complementary information on specific Wilson coefficients [23].

The LHCb measurement of the K and K^* isospin asymmetries in bins of q^2 are shown in Fig. 6. For the K^* modes A_I is compatible with the SM expectation that $A_I^{SM} \simeq 0$, but for the K^+/K^0 modes, A_I is seen to be negative at low- and high- q^2 [24]. Especially, the two q^2 bins below $4.3 \text{ GeV}^2/c^2$ and the highest bin above $16 \text{ GeV}^2/c^2$ have the most negative isospin asymmetry. These q^2 regions are furthest from the charmonium regions and are therefore cleanly predicted theoretically. This is consistent with what was seen at previous experiments, but is inconsistent with the naive expectation of $A_I \sim 0$ at the four sigma level.

2.3.3 $B_s^0 \rightarrow \phi \mu^+ \mu^-$

The $B_s^0 \rightarrow \phi \mu^+ \mu^-$ decay is also sensitive to new physics through angular observables but for the time being, the available statistics does not allow an angular analysis. However, with 1.0 fb^{-1} of data, LHCb observes 77 ± 10 candidates [25]. Normalizing to the $B_s^0 \rightarrow J/\psi \phi$ channel, the branching ratio is measured to be $BR(B_s^0 \rightarrow \phi \mu^+ \mu^-) = (0.78 \pm 0.10_{stat} \pm 0.06_{syst} \pm 0.28_{BR}) \times 10^{-6}$, which is compatible with the previous CDF measurement [26]. LHCb also obtains the differential branching fractions in q^2 bins as shown in Fig. 7.

2.3.4 $B^+ \rightarrow \pi^+ \mu^+ \mu^-$

In the 2011 data sample, the very rare decay $B^+ \rightarrow \pi^+ \mu^+ \mu^-$ was observed at the LHCb experiment for the first time. This is the rarest B decay ever observed. It is a $b \rightarrow d \ell^+ \ell^-$ transition, which in the SM is suppressed by loop and CKM factors proportional to $|V_{td}|/|V_{ts}|$. In the 1.0

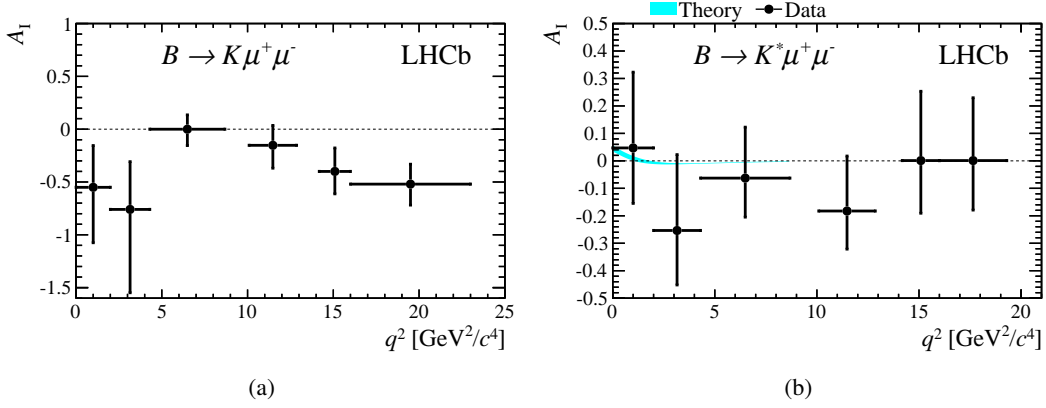


Figure 6: $B \rightarrow K\mu^+\mu^-$ (a) and $B \rightarrow K^*\mu^+\mu^-$ isospin asymmetries in 1.0 fb⁻¹ of data collected by the LHCb collaboration in 2011 [24].

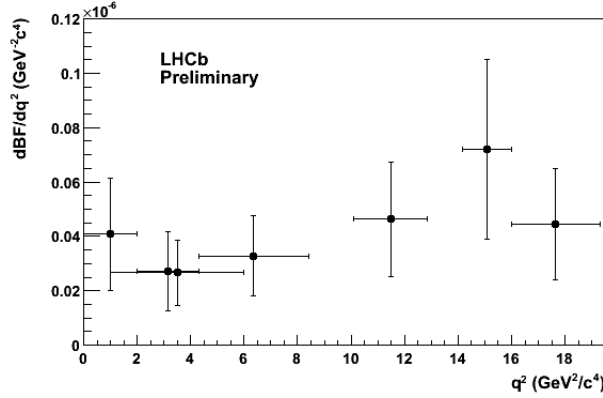


Figure 7: $BR(B_s^0 \rightarrow \phi\mu^+\mu^-)$ as a function of q^2 from Ref. [25]. The errors are the combined statistical and systematic uncertainties.

fb⁻¹ data sample, LHCb observes $25.3^{+6.7}_{-6.4}$ signal candidates, as shown in Fig.8, corresponding to a branching fraction of $\mathcal{B}(B^+ \rightarrow \pi^+\mu^+\mu^-) = 2.3 \pm 0.6 \pm 0.1 \times 10^{-8}$ [27]. This measurement is in good agreement with the SM prediction, which is consistent with there being no large NP contribution to the $b \rightarrow d\ell^+\ell^-$ processes and with the MFV hypothesis.

The $b \rightarrow d$ transitions can show potentially larger CP and isospin violating effects than their $b \rightarrow s$ counterparts due to the different CKM hierarchy [21]. These studies would need the large statistics provided by the future LHCb Upgrade.

2.3.5 Rare radiative decays

In 1.0 fb⁻¹ of integrated luminosity LHCb observes $5279 \pm 93 B^0 \rightarrow K^{*0}\gamma$ and $691 \pm 36 B_s^0 \rightarrow \phi\gamma$ candidates, respectively [28]. These are the largest samples of rare radiative B^0 and B_s^0 decays collected by a single experiment. The large sample of $B^0 \rightarrow K^{*0}\gamma$ decays has enabled LHCb to make the world's most precise measurement of the direct CP -asymmetry $A_{CP}(K^*\gamma) = 0.8 \pm 1.7 \pm 0.9\%$ [28]. This value is compatible with the SM expectation $A_{CP}(K^*\gamma) = -0.0061 \pm 0.0043$ [29].

With more statistics, LHCb can perform more analyses of radiative decays, in order to add ad-

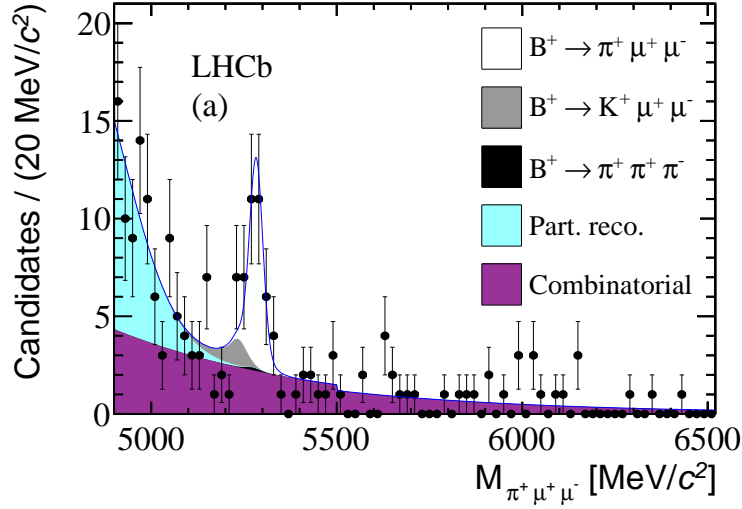


Figure 8: The $\pi^+\mu^+\mu^-$ invariant mass of selected $B^+ \rightarrow \pi^+\mu^+\mu^-$ candidates in 1.0 fb^{-1} of integrated luminosity [27]. In the legend, “part. reco.” and “combinatorial” refer to partially reconstructed and combinatorial background respectively.

ditional constraints on the $C_7 - C_7'$ plane through measurements of $b \rightarrow s\gamma$ processes. This includes a time-dependent analysis of $B_s^0 \rightarrow \phi\gamma$, and measurements of the photon polarisation through the decays $\Lambda_b^0 \rightarrow \Lambda^{(*)}\gamma$.

2.3.6 Model-independent analysis of new physics contributions

The experimental results presented before can be used to put direct constraints on the Wilson coefficients in a model-independent way. Several studies have been done, for example the one in Fig. 9, taken from Ref. [30], which shows the current constraints on NP contributions to the Wilson coefficients $C_7^{(\prime)}$, $C_9^{(\prime)}$ and $C_{10}^{(\prime)}$, varying only one coefficient at a time.

The experimental constraints included here are: the branching fractions of $B \rightarrow X_s\gamma$, $B \rightarrow X_s\ell^+\ell^-$, $B \rightarrow K\mu^+\mu^-$ and $B_s \rightarrow \mu^+\mu^-$, the time-dependent CP asymmetries in $B \rightarrow K^*\gamma$ and $b \rightarrow s\gamma$, and the branching fraction and angular observables in $B \rightarrow K^*\mu^+\mu^-$. One can make the following observations:

- At 95% C.L., all Wilson coefficients are compatible with their SM values.
- For the Wilson coefficients $C_{10}^{(\prime)}$, the latest constraint on $\mathcal{B}(B_s^0 \rightarrow \mu^+\mu^-)$ is starting to become competitive with the constraints from the angular analysis of $B \rightarrow K^{(*)}\mu^+\mu^-$.
- The constraints on C_9' and C_{10}' from $B \rightarrow K\mu^+\mu^-$ and $B \rightarrow K^*\mu^+\mu^-$ are complementary and lead to a more constrained region, and better agreement with the SM, than with $B \rightarrow K^*\mu^+\mu^-$ alone.
- A second allowed region in the $C_7 - C_7'$ plane characterised by large positive contributions to both coefficients, which was found previously to be allowed *e.g.* in Refs. [31, 32], is now disfavoured at 95% C.L. by the new $B \rightarrow K^*\mu^+\mu^-$ data, in particular the measurements of the forward-backward asymmetry from LHCb.

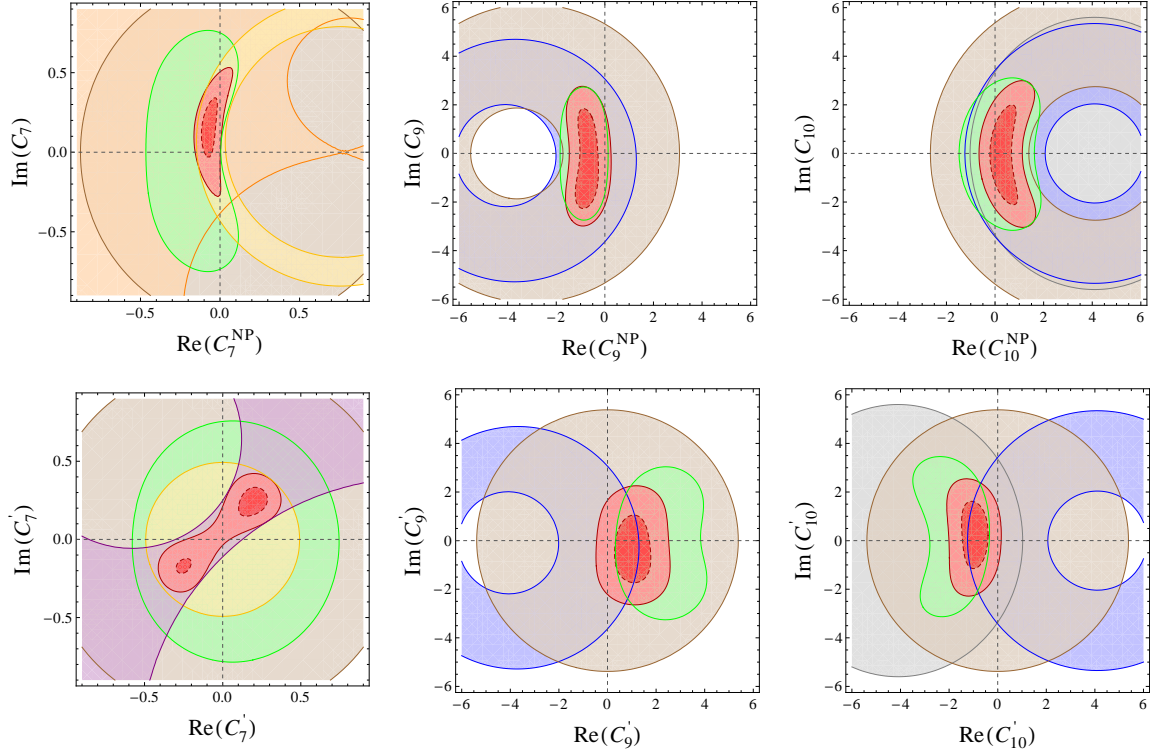


Figure 9: Individual 2σ constraints in the complex planes of Wilson coefficients, coming from $B \rightarrow X_s \ell^+ \ell^-$ (brown), $B \rightarrow X_s \gamma$ (yellow), $A_{CP}(b \rightarrow s \gamma)$ (orange), $B \rightarrow K^* \gamma$ (purple), $B \rightarrow K^* \mu^+ \mu^-$ (green), $B \rightarrow K \mu^+ \mu^-$ (blue), and $B_s \rightarrow \mu^+ \mu^-$ (grey), as well as combined 1 and 2σ constraints (red). Figure taken from Ref. [30].

Significant improvements of these constraints – or first hints for physics beyond the SM – can be obtained in the future by both improved measurements of the observables discussed above and by improvements on the theoretical side.

3. CP violation

Although the current observed CP violation phenomena are well described in the SM by the CKM mechanism, the SM is not able to explain the observed baryon asymmetry of the universe. Thus, new sources of CP violation should exist. An interesting place to look for new CP violation sources is the b hadron system in which new particles can enter the loop mediated processes, modifying the value of CP observables with respect to their SM expectations. In particular, LHCb can exploit the large number of B_s^0 meson and charm hadrons produced in pp collisions.

3.1 B_s^0 mixing observables

3.1.1 Measurement of Δm_s

The mass difference between the heavy and light B_s^0 mass eigenstate, Δm_s , is measured by LHCb with 0.34 fb^{-1} of data [33]. In this analysis, 9189 B_s^0 candidates are reconstructed with the decay channel $B_s^0 \rightarrow D_s^- \pi^+$. The oscillation frequency is measured using a unbinned maximum likelihood fit based on the reconstructed B_s^0 mass, its decay time, and the information from opposite

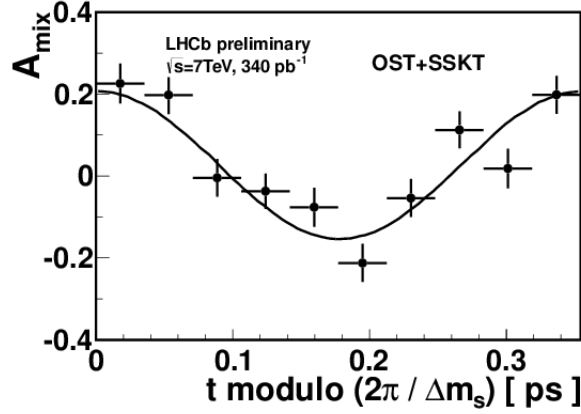


Figure 10: Mixing asymmetry for B_s^0 signal candidates as function of the decay time, modulo $2\pi/\Delta m_s$ [33]. The fitted signal asymmetry is superimposed.

side and same side tagging algorithms. The same side tagger exploits the extra particle produced at the fragmentation process of the signal B : a pion in the case of B^0 or B^+ signal and a kaon for B_s^0 . The opposite side taggers use the decay products of the other b-hadron produced in the event. The obtained value for Δm_s is $17.725 \pm 0.041 \pm 0.026 \text{ ps}^{-1}$. It is the world best measurement and is compatible with the SM expectation of $\Delta m_s = 17.3 \pm 2.6 \text{ ps}^{-1}$ [34].

To illustrate the oscillation pattern, we can use the time dependent mixing amplitude, defined as:

$$A_{\text{mix}}(t) = \frac{N(B_s^0; q = +1)(t) - N(B_s^0; q = -1)(t)}{N(B_s^0; q = +1)(t) + N(B_s^0; q = -1)(t)} \quad (3.1)$$

where $N(B_s^0; q = +1)(t)$ and $N(B_s^0; q = -1)(t)$ are the numbers of mass-sideband subtracted B_s^0 signal candidates with a given decay time t and the tagging decision $+1$ and -1 respectively. Despite the limited statistics of the sample, the oscillation pattern is clearly visible when the amplitude is plotted as function of the decay time, folded according to modulo $2\pi/\Delta m_s$ (Fig.10).

3.1.2 Measurement of ϕ_s

The CP violating phase in B_s^0 mixing, ϕ_s , appears in the interference between a direct decay to a final state and the decay to the same final state after oscillation. It is related to the Unitarity Triangle angle by $\phi_s \approx -2\beta_s$, with $\beta_s \equiv \arg(-\frac{V_{ts}V_{tb}^*}{V_{cb}V_{cs}^*})$. It has a very precise SM prediction: $\phi_s^{SM} = 0.036 \pm 0.002 \text{ rad}$ [34, 35]. LHCb measures this phase, simultaneously with the decay width difference $\Delta\Gamma_s$, in the $B_s^0 \rightarrow J\psi\phi$ channel. Because the final state is a mixing of CP odd and even final state, it requires a full angular analysis, in addition of being time dependent and tagged, which makes it particularly complex. Analysing 1.0 fb^{-1} of data, LHCb finds 21200 $B_s^0 \rightarrow J\psi\phi$ candidates and measures [8] :

$$\phi_s = -0.001 \pm 0.101 \pm 0.027 \text{ rad}, \quad \Delta\Gamma_s = 0.116 \pm 0.018 \pm 0.006 \text{ ps}^{-1}. \quad (3.2)$$

The ambiguous solution corresponding to ($\phi_s \leftrightarrow \pi - \phi_s$, $\Delta\Gamma_s \leftrightarrow -\Delta\Gamma_s$) has been ruled out by a study from LHCb which determined the sign of $\Delta\Gamma_s$ to be positive at 4.7σ confidence level [37] by exploiting the interference between the K^+K^- S-wave and P-wave amplitudes in the $\phi(1020)$

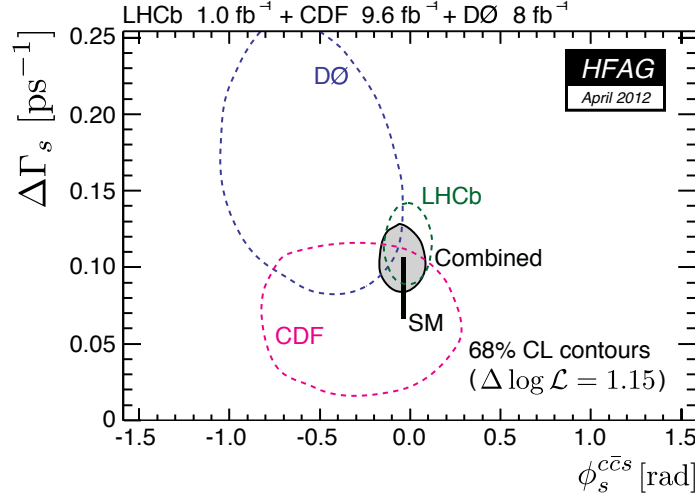


Figure 11: HFAG 2012 combination of ϕ_s and $\Delta\Gamma_s$ results, where the 1σ confidence region is shown for each experiment and the combined result [36].

mass region as proposed in [38]. This resolved the two-fold ambiguity in the value of ϕ_s for the first time.

LHCb has also studied $B_s^0 \rightarrow J/\psi \pi^+ \pi^-$. The $\pi^+ \pi^-$ mass range 775–1550 MeV is used for the measurement, where ~ 7400 candidates are found using 1.0 fb^{-1} . This region of mass, around the f_0 , gives a CP -odd final state, so there is no need to do an angular analysis. Using as input the value of $\Delta\Gamma_s$ obtained from $B_s^0 \rightarrow J/\psi \phi$, the measurement from the analysis of $B_s^0 \rightarrow J/\psi \pi^+ \pi^-$ is [39]

$$\phi_s = -0.019_{-0.174-0.003}^{+0.173+0.004} \text{ rad}. \quad (3.3)$$

Both measurements of ϕ_s are compatible within uncertainties. They were combined in a simultaneous fit resulting in :

$$\phi_s = -0.002 \pm 0.083 \pm 0.027 \text{ rad}. \quad (3.4)$$

The results of different experiments as well as the HFAG average [36] are shown in Fig. 11, and are in good agreement with the SM expectations.

As the experimental determination of ϕ_s is expected to improve in the coming years, it becomes important to evaluate the pollution due to penguins contribution as suggested by [40].

3.2 CP violation in the charm sector

LHCb has recently found a first evidence of CP violation in the charm sector, measuring $\Delta\mathcal{A}_{CP}$ which is defined as:

$$\begin{aligned} \Delta\mathcal{A}_{CP} &\equiv A_{CP}(K^+K^-) - A_{CP}(\pi^+\pi^-) = a_{CP}^{\text{dir}}(K^+K^-) - a_{CP}^{\text{dir}}(\pi^+\pi^-) \\ &\approx \Delta a_{CP}^{\text{dir}} \left(1 + y \cos \phi \frac{\langle t \rangle}{\tau} \right) + \left(a_{CP}^{\text{ind}} + \overline{a_{CP}^{\text{dir}}} y \cos \phi \right) \frac{\Delta\langle t \rangle}{\tau}. \end{aligned} \quad (3.5)$$

The ratio $\Delta\langle t \rangle/\tau$ is 0.098 ± 0.003 for LHCb, therefore $\Delta\mathcal{A}_{CP}$ is largely a measure of direct CP violation. Measuring the difference between the $D^0 \rightarrow K^+K^-$ and $D^0 \rightarrow \pi^+\pi^-$ channel allows

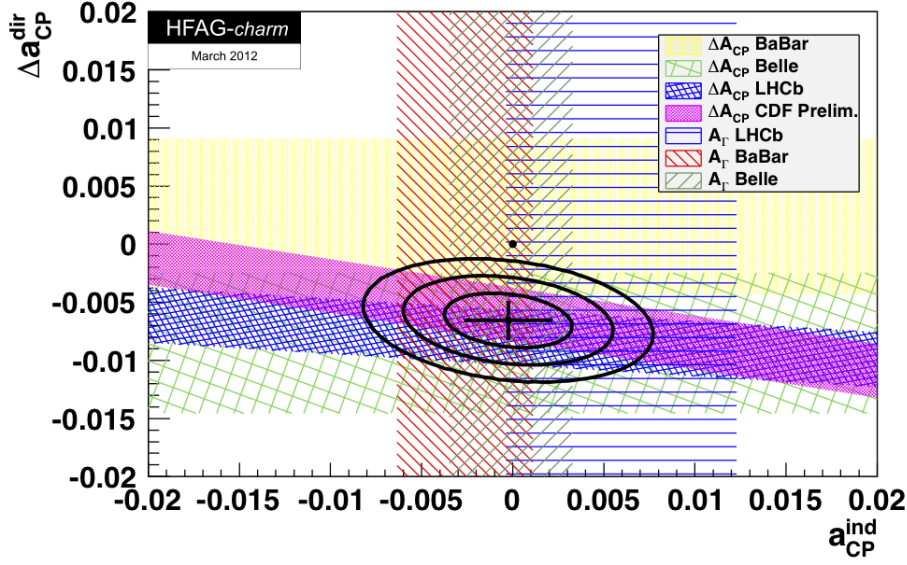


Figure 12: HFAG 2012 combination of $\Delta\mathcal{A}_{CP}$ and a_{CP}^{ind} . The band represent 1σ interval, the point of no CP violation is shown as a filled circle and two-dimensional 68% CL, 95% CL, and 99.7% CL regions are plotted as ellipses with the best fit value as a cross indicating the one-dimensional uncertainties in their center [36].

to minimize experimental systematic uncertainties. LHCb measures: $\Delta\mathcal{A}_{CP} = (-0.82 \pm 0.21 \pm 0.11)\%$ [41]. CDF confirmed this measurement finding: $\Delta\mathcal{A}_{CP} = (-0.62 \pm 0.21 \pm 0.10)\%$ [42]. The HFAG combination is shown in Fig12, the world average⁴ is consistent with no CP violation at only 0.006% C.L. [36].

This evidence for non-zero CP violation raises the question of its interpretation in the SM, where enhanced penguin amplitudes could explained this result. The situation from the theory side is not clear as computation of these penguin amplitudes is difficult. Work is ongoing to improve both SM expectation and possible NP contribution.

3.3 Measurement of the Unitarity Triangle angle γ

The CKM angle γ , defined as the phase $\gamma = \arg[-V_{ud}V_{ub}^*/(V_{cd}V_{cb}^*)]$, is the least well known parameter of the Unitarity Triangle⁵. The average of the experimental measurements has an uncertainty of the order of 11-12°, while the indirect constraints from the Unitarity Triangle fit gives a value of $\gamma = (68.5 \pm 3.2)^\circ$ from the UTfit collaboration [43] and $\gamma = (67.1 \pm 4.3)^\circ$ from the CKMfitter collaboration [44].

γ can be determined from tree-mediated processes, which are theoretically very clean, or loop-mediated processes. Several established methods to measure γ in tree decays exploit the $B^- \rightarrow D^{(*)}K^{(*)-}$ decays. They are based on the interference between the $b \rightarrow u$ and $b \rightarrow c$ tree amplitudes, which arises when the neutral D meson is reconstructed in a final state accessible to both D^0 and \bar{D}^0 decays. The interference between the amplitudes results in observables that depend on their

⁴New results presented by Belle at ICHEP 2012 are not included in this average.

⁵For a detailed review of the Unitarity Triangle status, see the talk of C. Tarantino at this conference.

relative weak phase γ . Besides γ , they also depend on hadronic parameters, namely the ratio of magnitudes of amplitudes $r_B \equiv |A(b \rightarrow u)/A(b \rightarrow c)|$ and the relative strong phase δ_B between the two amplitudes. These hadronic parameters depend on the B decay under investigation. They can not be precisely calculated from theory, but can be extracted directly from data by simultaneously reconstructing several different D final states.

There are three main techniques to determine γ , that depend on the given D final state:

- The GLW method [45, 46] uses a CP eigenstate for the D decay. It provides a set of four observables that are connected to the three unknowns γ , r_B , and δ_B through

$$R_{CP\pm} = 1 + r_B^2 \pm 2r_B \cos \delta_B \cos \gamma \quad (3.6)$$

$$A_{CP\pm} = \frac{\pm 2r_B \sin \delta_B \sin \gamma}{R_{CP\pm}}. \quad (3.7)$$

- The ADS method [47, 48], in which the D mesons are selected in Cabibbo allowed and doubly Cabibbo suppressed decays, such as $D^0 \rightarrow K^- \pi^+$ and $D^0 \rightarrow \pi^- K^+$, respectively. In that case the measured observables are related to the unknown γ , r_B , r_D , δ_B and δ_D through

$$R_{\text{ADS}} = r_B^2 + r_D^2 + 2r_B r_D \cos \gamma \cos(\delta_B + \delta_D) \quad (3.8)$$

$$A_{\text{ADS}} = 2r_B r_D \sin \gamma \sin(\delta_B + \delta_D) / R_{\text{ADS}} \quad (3.9)$$

- The GGSZ method [49], that uses a three body self-conjugate decay for the D , as $D \rightarrow K_s^0 \pi^+ \pi^-$ or $D \rightarrow K_s^0 K^+ K^-$ and requires a Dalitz plot-based analysis.

Besides the established methods based on direct CP violation in $B \rightarrow DK$ decays, it is also possible to measure γ using time-dependent analyses of neutral B^0 and B_s^0 tree decays [50, 51, 52]. It is clear that the best sensitivity to γ result from the combination of the results from different methods.

A particularly interesting result has been obtained by LHCb for $B^- \rightarrow DK^-$ with the GLW and ADS final states [53]. Analysing 1 fb^{-1} of data, the $B^\pm \rightarrow DK^\pm$ ADS mode is observed with $\sim 10\sigma$ statistical significance. This mode displays evidence (4.0σ) of a large negative asymmetry, as can be seen on Fig 13, consistent with previous experiments. The direct CP violation in $B^\pm \rightarrow DK^\pm$ decays is observed with a significance of of 5.8σ .

This example shows that LHCb is competitive with the B factories and the Tevatron for the γ measurement. Many other analyses have been, and are being, done by LHCb. For a more complete review see Ref. [54]. A new γ measurement has also been done from a combination of $B^+ \rightarrow Dh^+$ analyses [55].

4. Spectroscopy

Recently, LHCb has reported the first observation of the Λ_b^{0*} [56]. The quark model predicts the existence of two orbitally excited Λ_b^0 states, Λ_b^{0*} , with the quantum numbers $J^P = 1/2^-$ and $3/2^-$ that should decay to $\Lambda_b^0 \pi^+ \pi^-$ or $\Lambda_b^0 \gamma$.

Analysing 1 fb^{-1} of data, two narrow states are observed in the $\Lambda_b^0 \pi^+ \pi^-$ spectrum with masses $5911.95 \pm 0.12 \pm 0.03 \pm 0.66 \text{ MeV}/c^2$ and $5919.76 \pm 0.07 \pm 0.02 \pm 0.66$, where the first error is

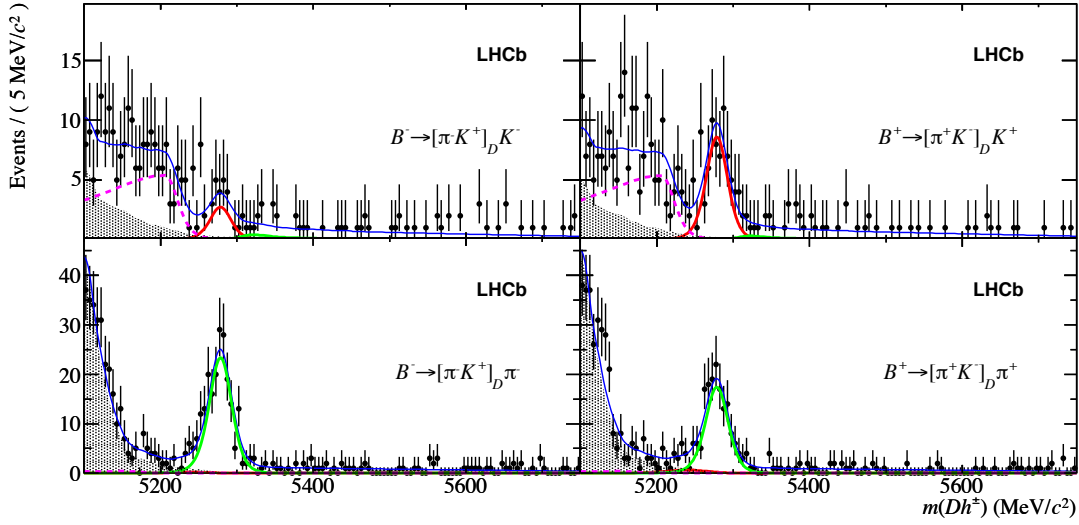


Figure 13: Invariant mass distributions of selected $B^\pm \rightarrow [\pi^\pm K^\pm]_D h^\pm$ candidates [53]: (left) B^- candidates, (right) B^+ candidates. In the top plots, the bachelor track passes a kaon PID cut and the B candidates are reconstructed assigning this track the kaon mass. The remaining events are placed in the bottom row and are reconstructed with a pion mass hypothesis. The dark (red) curve represents the $B \rightarrow DK^\pm$ events, the light (green) curve is $B \rightarrow D\pi^\pm$. The shaded contribution are partially reconstructed events and the thin line shows the total PDF which also includes a linear combinatoric component. The broken line represents the partially reconstructed, but Cabibbo favoured, $\bar{B}_s^0 \rightarrow D^0 K^+ \pi^-$ decays where the pion is lost.

statistical, the second is systematic, and the third one is the uncertainty due to the knowledge of the Λ_b^0 mass. The corresponding significance are 4.9 and 10.1σ respectively. These two states are clearly seen on Fig.14. They are interpreted as orbitally-excited Λ_b^0 baryons, $\Lambda_b^{0*}(5912)$ and $\Lambda_b^{0*}(5920)$

Another interesting analysis concerns the search for excited B states. Looking at the $B^+ K^-$, $B^+ \pi^-$ and $B^0 \pi^+$ final states in 0.34 fb^{-1} of data, LHCb observes peaks that correspond to $B_{(s)1}$ and $B_{(s)2}^*$ resonances with greater than 5σ significance in all cases except for $B_2^{*+} \rightarrow B^0 \pi^+$, where we have evidence of a peak at more than 3σ [57]. This is the first observation (evidence) of the $B_1^+ \rightarrow B^{0*} \pi^+$ ($B_2^{*+} \rightarrow B^0 \pi^+$) decay. The corresponding masses are measure to be

$$\begin{aligned}
 M_{B_{s1}^0} &= (5828.99 \pm 0.08_{\text{stat}} \pm 0.13_{\text{syst}} \pm 0.45_{\text{syst}}^{B_{\text{mass}}}) \text{ MeV}/c^2, \\
 M_{B_{s2}^{*0}} &= (5839.67 \pm 0.13_{\text{stat}} \pm 0.17_{\text{syst}} \pm 0.29_{\text{syst}}^{B_{\text{mass}}}) \text{ MeV}/c^2, \\
 M_{B_1^0} &= (5724.1 \pm 1.7_{\text{stat}} \pm 2.0_{\text{syst}} \pm 0.5_{\text{syst}}^{B_{\text{mass}}}) \text{ MeV}/c^2, \\
 M_{B_1^+} &= (5726.3 \pm 1.9_{\text{stat}} \pm 3.0_{\text{syst}} \pm 0.5_{\text{syst}}^{B_{\text{mass}}}) \text{ MeV}/c^2, \\
 M_{B_2^{*0}} &= (5738.6 \pm 1.2_{\text{stat}} \pm 1.2_{\text{syst}} \pm 0.3_{\text{syst}}^{B_{\text{mass}}}) \text{ MeV}/c^2, \\
 M_{B_2^{*+}} &= (5739.0 \pm 3.3_{\text{stat}} \pm 1.6_{\text{syst}} \pm 0.3_{\text{syst}}^{B_{\text{mass}}}) \text{ MeV}/c^2,
 \end{aligned}$$

where the third source of uncertainty is from the B mass uncertainty. All masses are in good agreement with theoretical predictions.

Many other spectroscopy analyses have been performed at LHCb. In particular, LHCb has the

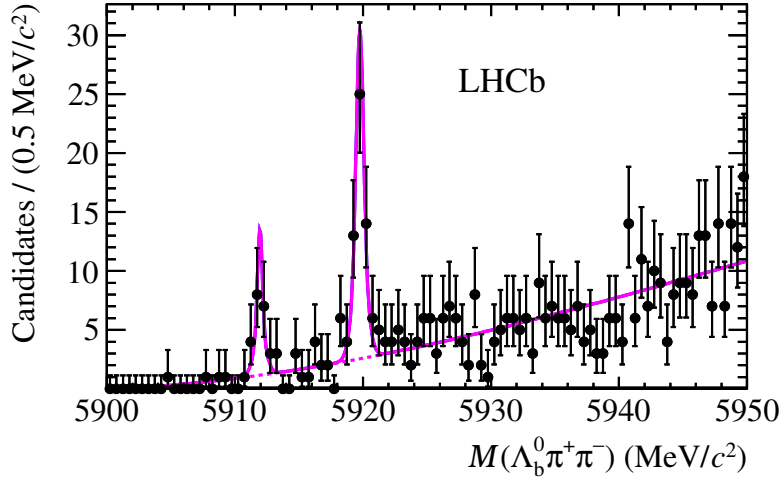


Figure 14: Invariant mass spectrum of $\Lambda_b^0 \pi^+ \pi^-$ combinations from Ref. [56]. The solid line is the fit result and the dashed line shows the background contribution.

world best measurement of B^+ , B^0 , B_s^0 , and Λ_b masses [58]. We also performed measurement of the B_c mass [59], and b baryon masses [60]. In addition, LHCb performed searches for exotic onia, as example the X(4140) [61] and the X(3872) [62].

5. The LHCb Upgrade

As we have seen from the main LHCb results presented here, new physics has not shown itself clearly, and deviation from SM predictions should be small. In this context it is essential to improve measurements of precisely predicted quantities. This is the goal of the LHCb Upgrade that will allow the experiment to run at the luminosity of $\mathcal{L}_{\text{inst}} = 10^{33}/\text{cm}^2/\text{s}$, collecting 5 fb^{-1} per year, with the final aim to collect a large data sample of 50 fb^{-1} . It is foreseen to be installed during the long shutdown 2 between 2017 and 2019, at the same time as the ATLAS and CMS upgrades.

With the current LHCb detector, the main limitation that prevents exploiting higher luminosity is the hardware trigger limiting the output rate to 1 MHz. The LHCb Upgrade proposal consists in removing the hardware trigger and reading out the entire detector at the 40 MHz crossing rate. This flexible software-based trigger strategy will allow to double the efficiency of the hadron, photon and electron triggers.

With this final dataset, one can expect a precision better than 10% on $\mathcal{B}(B_s^0 \rightarrow \mu^+ \mu^-)$ and $\sim 35\%$ on the ratio $\mathcal{B}(B_s^0 \rightarrow \mu^+ \mu^-)/\mathcal{B}(B^0 \rightarrow \mu^+ \mu^-)$, assuming the SM value for the branching ratios. Concerning CP violation and mixing, with the LHCb Upgrade we could reach an uncertainty on ϕ_s of 0.008 with the $B_s^0 \rightarrow J/\psi \phi$ channel, and a precision on γ of $\sim 0.9^\circ$ combining the tree level decays.

For a detailed discussion about the LHCb Upgrade see Ref. [63] and [64].

6. Conclusion

A selection of recent LHCb results has been shown. The excellent physics reach of LHCb, al-

ready competitive with, or better than, the B factories and Tevatron experiments in a large number of analysis, have been possible thanks to the excellent performances of the LHC and the detector in the past two years. Despite a lot of effort to search for new physics in various decay modes and observables, large effects have been ruled out in the flavour sector. However, the potential for discovery of physics beyond the Standard Model is still very high in this sector and the experimental precision as well as the theoretical cleanliness of the observables are now the most important parameters in the game.

For a more complete review of the LHCb results and their implication on the search for new physics, see [54].

7. Acknowledgements

I would like to thank the organisers of the Lattice 2012 conference for their invitation.

References

- [1] R. Aaij *et al.* [LHCb Collaboration], *Measurement of $\sigma(pp \rightarrow b\bar{b}X)$ at $\sqrt{s} = 7$ TeV in the forward region*, Phys. Lett. **B694** (2010) 209, [arXiv:1009.2731].
- [2] R. Aaij *et al.* [LHCb Collaboration], *Prompt charm production in pp collisions at $\sqrt{s} = 7$ TeV*, LHCb-CONF-2010-013.
- [3] A. J. Buras, *et al.*, *Higgs-mediated FCNCs: Natural Flavour Conservation vs. Minimal Flavour Violation*, JHEP **1010** (2010) 009, [arXiv:1005.5310].
- [4] J. Laiho, E. Lunghi, and R. Van de Water, *Lattice QCD inputs to the CKM unitarity triangle analysis*, Phys. Rev. **D81** (2010) 034503, [arXiv:0910.2928], updated results and plots available at: <http://www.latticeaverages.org/>.
- [5] A. J. Buras, J. Girrbach, *BSM models facing the recent LHCb data: A First look*, [arXiv:1204.5064].
- [6] K. De Bruyn *et al.*, *A New Window for New Physics in $B_s^0 \rightarrow \mu^+ \mu^-$* , [arXiv:1204.1737].
- [7] K. De Bruyn *et al.*, *On Branching Ratio Measurements of B_s Decays*, Phys. Rev. Lett. **109** (2012) 04801, [arXiv:1204.1735].
- [8] R. Aaij *et al.* [LHCb Collaboration], *Tagged time-dependent angular analysis of $B_s^0 \rightarrow J/\psi\phi$ decays at LHCb*, LHCb-CONF-2012-002.
- [9] R. Aaij *et al.* [LHCb Collaboration], *Determination of f_s/f_d for 7 TeV pp collisions and a measurement of the branching fraction of the decay $B_d \rightarrow D^- K^+$* , Phys. Rev. Lett. **107** (2011) 211801, [arXiv:11106.4435].
- [10] R. Aaij *et al.* [LHCb Collaboration], *Measurement of b-hadron production fractions in 7 TeV pp collisions*, Phys. Rev. **D85** (2012) 032008, [arXiv:1111.2357].
- [11] R. Aaij *et al.* [LHCb Collaboration], *Average f_s/f_d b-hadron production fraction for 7 TeV pp collision at LHCb*, LHCb-CONF-2011-034.
- [12] A. Bailey *et al.*, *$B_s \rightarrow D_s / B \rightarrow D$ semileptonic form-factors ratios and their application to $B_s^0 \rightarrow \mu^+ \mu^-$* , Phys. Rev. **D85** (2012) 114502, [arXiv:1202.6346].
- [13] R. Aaij *et al.* [LHCb Collaboration], *Strong constraint on the rare decays $B_s^0 \rightarrow \mu^+ \mu^-$ and $B^0 \rightarrow \mu^+ \mu^-$* . Phys. Rev. Lett. **108** (2012) 231801, [arXiv:1203.4493].

- [14] ATLAS, CMS and LHCb collaborations, *Search for the rare decays $B_{(s)}^0 \rightarrow \mu^+ \mu^-$ at the LHC with the ATLAS, CMS and LHCb experiments*, LHCb-CONF-2012-017.
- [15] Mahmoudi, F., *Direct and indirect searches for New Physics*, Proceeding of Moriond QCD 2012 [arXiv:1205.3099].
- [16] W. Altmannshofer, A. J. Buras, S. Gori, P. Paradisi, and D. M. Straub, *Anatomy and Phenomenology of FCNC and CPV Effects in SUSY Theories*, Nucl. Phys. **B830** (2010) 17-94, [arXiv:0909.1333].
- [17] R. Aaij *et al.* [LHCb Collaboration], *Differential branching fraction and angular analysis of the $B^0 \rightarrow K^* \mu^+ \mu^-$ decay*, LHCb-CONF-2012-008.
- [18] C. Bobeth and G. Hiller, and G. Piranishvili, *CP Asymmetries in $\bar{B} \rightarrow \bar{K}^* (\rightarrow \bar{K} \pi) \bar{\ell} \ell$ and Untagged $\bar{B}_s, B_s \rightarrow \phi (\rightarrow K^+ K^-) \bar{\ell} \ell$ Decays at NLO*, JHEP **0807** (2008) 106, [arXiv:0805.2525].
- [19] C. Bobeth and G. Hiller, and D. van Dyk, *More Benefits of Semileptonic Rare B Decays at Low Recoil: CP Violation*, JHEP **1107** (2011) 1107, [arXiv:1105.0376].
- [20] C. Bobeth and G. Hiller, and D. van Dyk, *The Decay $\bar{B} \rightarrow \bar{K} \ell^+ \ell^-$ at Low Hadronic Recoil and Model-Independent $\Delta B = 1$ Constraints*, JHEP **1201** (2012) 1207, [arXiv:1111.2558].
- [21] M. Beneke, Th. Feldmann, and D. Seidel, *Exclusive radiative and electroweak $b \rightarrow d$ and $b \rightarrow s$ penguin decays at NLO*, Eur. Phys. J. **C41** (2005) 173-188, [arXiv:hep-ph/041240].
- [22] Ali, A. and Kramer, G. and Zhu, Guo-huai, *$B \rightarrow K^* \ell^+ \ell^-$ decay in soft-collinear effective theory*, Eur. Phys. J. **C47** (2006) 625-641 [arXiv:hep-ph/0601034]
- [23] T. Feldmann and J. Matias, *Forward backward and isospin asymmetry for $B \rightarrow K^* \ell^+ \ell^-$ decay in the standard model and in supersymmetry*, JHEP **0301** (2003) 0301, [arXiv:hep-ph/0212158]
- [24] R. Aaij *et al.* [LHCb Collaboration], *Measurement of the isospin asymmetry in $B \rightarrow K^{(*)} \mu^+ \mu^-$ decays*, JHEP **07** (2012) 133 [arXiv:1205.3422].
- [25] R. Aaij *et al.* [LHCb Collaboration], *Measurement of the ratio of branching fractions for $B_s^0 \rightarrow \phi \mu^+ \mu^-$ and $B_s^0 \rightarrow J/\psi \phi$* , LHCb-CONF-2012-003.
- [26] T. Aaltonen *et al.* [CDF Collaboration], *Observation of the Baryonic Flavor-Changing Neutral Current Decay $\lambda_b \rightarrow \lambda \mu \mu$* , Phys. Rev. Lett. **107** (2011) 201802, [arXiv:1107.3753]
- [27] R. Aaij *et al.* [LHCb Collaboration], *First observation of $B^+ \rightarrow \pi^+ \mu^+ \mu^-$* , submitted to JHEP, [arXiv:1210.2645].
- [28] R. Aaij *et al.* [LHCb Collaboration], *Measurement of the ratio of the branching fractions $\frac{\mathcal{B}(B_d^0 \rightarrow K^{*0} \gamma)}{\mathcal{B}(B_s^0 \rightarrow \phi \gamma)}$ and the direct CP asymmetry in $B_d^0 \rightarrow K^{*0} \gamma$* , Nucl. Phys. **B867** (2012) 1-18, [arXiv:1209.0317].
- [29] M. Matsumori, A. I. Sanda and Y. Keum, *CP asymmetry, branching ratios and isospin breaking effects of $B \rightarrow K^* \gamma$ with the perturbative QCD approach.*, Phys. Rev. **D72** (2005) 014013, [arXiv:hep-ph/0406055].
- [30] W. Altmannshofer and D. Straub, *Cornering New Physics in $b \rightarrow s$ Transitions*, [arXiv:1206.0273].
- [31] W. Altmannshofer, P. Paradisi, and D. Straub, *Model-Independent Constraints on New Physics in $b \rightarrow s$ Transitions*, JHEP **1204** (2012) 008, [arXiv:1111.1257].
- [32] S. Descotes-Genon *et al.*, *Exploring New Physics in the $C_7 - C_7'$ plane*, JHEP **1106** (2011) 099, [arXiv:1104.3342]
- [33] R. Aaij *et al.* [LHCb Collaboration], *Measurement of Δm_s in the decay $B_s^0 \rightarrow D_s^- (K^+ K^- \pi^-) \pi^+$ using opposite-side and same-side flavour tagging algorithms*, LHCb-CONF-2011-050.

- [34] A. Lenz and U. Nierste, *Numerical updates of lifetimes and mixing parameters of B mesons*, [arXiv:1102.4274].
- [35] J. Charles et al., *Predictions of selected avour observables within the Standard Model*, Phys. Rev. **D84** (2011) 033005, [arXiv:1106.4041].
- [36] Heavy Flavor Averaging Group, Y. Amhis *et al.*, <http://www.slac.stanford.edu/xorg/hfag/>.
- [37] R. Aaij *et al.* [LHCb Collaboration], *Determination of the sign of the decay width difference in the B_s^0 system*, Phys. Rev. Lett. **108**, (2012) 241801, [arXiv:1202.4717].
- [38] Y. Xie *et al.*, *Determination of $2\beta_s$ in $B_s^0 \rightarrow J/\psi K^+K^-$ Decays in the Presence of a K^+K^- S-Wave Contribution*, JHEP **0909** (2009) 074, [arXiv:0908.3627].
- [39] R. Aaij *et al.* [LHCb Collaboration], *Measurement of the CP-violating phase ϕ_s in $\bar{B}_s^0 \rightarrow J/\psi \pi^+ \pi^-$ decays.*, Phys. Lett. **B73** (2012) 378-386, [arXiv:1204.5675].
- [40] S.Faller, R. Fleischer, T. Mannel, *Precision Physics with $B_s^0 \rightarrow J/\psi \phi$ at the LHC: The Quest for New Physics*, Phys. Rev. **D79** (2009) 014005, [arXiv:0810.4248].
- [41] R. Aaij *et al.* [LHCb Collaboration], *Evidence for CP violation in time-integrated $D^0 \rightarrow h^- h^+$ decay rates*, Phys. Rev. Lett. **108** (2012) 111602, [arXiv:1112.0938].
- [42] CDF collaboration, *Measurement of the difference in CP violating asymmetry between $D^0 \rightarrow KK$ and $D^0 \rightarrow \pi\pi$* , CDF Public Note 10784, Feb 2012.
- [43] UTfit collaboration, <http://www.utfit.org>.
- [44] CKMFitter collaboration, <http://ckmfitter.in2p3.fr/>.
- [45] M. Gronau and D. London, *How to determine all the angles of the unitarity triangle from $B^0 \rightarrow DK_s^0$ and $B_s^0 \rightarrow D\phi$* , Phys. Lett. **B253** (1991) 483-488,
- [46] M. Gronau and D. Wyler, *On determining a weak phase from CP asymmetries in charged B decays*, Phys. Lett. **B265** (1991) 172-176.
- [47] D. Atwood, I. Dunietz and A. Soni, *Enhanced CP violation with $B \rightarrow KD^0$ (\bar{D}^0) modes and extraction of the CKM angle γ* , Phys. Rev. Lett. **78** (1997) 3257-3260, [arXiv:hep-ph/9612433].
- [48] D. Atwood, I. Dunietz and A. Soni, *Improved methods for observing CP violation in $B^\pm \rightarrow KD$ and measuring the CKM phase γ* , Phys. Rev. **D63** (2001) 036005, [arXiv:hep-ph/0008090].
- [49] A. Giri *et al.*, *Determining γ using $B^\pm \rightarrow DK^\pm$ with multibody D decays*, Phys. Rev. **D68** (2003) 054018, [arXiv:hep-ph/0303187].
- [50] I. Dunietz and R. Sachs, *Asymmetry between inclusive charmed and anticharmed mopedes in B^0, \bar{B}^0 decay as a measure of CP violation*, Phys. Rev. **D37** (1988) 3186.
- [51] R. Aleksan, I. Dunietz and B. Kayser, *Determining the CP violating phase γ* , Z. Phys. **C54** (1992) 653-660.
- [52] R. Fleischer, *New strategies to obtain insights into CP violation through $B_s^0 \rightarrow D_s^\pm K^\mp, D_s^{*\pm} K^\mp, \dots$ and $B^0 \rightarrow D^\pm \pi^\mp, D_s^\pm \pi^\mp, \dots$ decays*, Nucl.Phys. **B671** 459-482, [arXiv:hep-ph/0304027]
- [53] R. Aaij *et al.* [LHCb Collaboration], *Obsevation of CP violation in $B^+ \rightarrow DK^+$ decays*, Phys. Lett. **B712** (2012) 203, [arXiv:1203.3662].
- [54] LHCb Collaboration and A. Bharucha, *et al.*, *Implications of LHCb measurements and future prospects*, LHCb-PUB-2012-006, [arXiv:1208.3355].

- [55] R. Aaij *et al.* [LHCb Collaboration], *A measurement of γ from a combination of $B^+ \rightarrow Dh^+$ analyses*, LHCb-CONF-2012-032.
- [56] R. Aaij *et al.* [LHCb Collaboration], *Observation of excited Λ_b^0 baryons*, submitted to Phys. Rev. Lett. [arXiv:1205.3452].
- [57] R. Aaij *et al.* [LHCb Collaboration], *Observations of Orbitally Excited $B_{(s)}^{**}$ Mesons*, LHCb-CONF-2011-053.
- [58] R. Aaij *et al.* [LHCb Collaboration], *Measurement of b -hadron masses*, Phys. Lett. **B708** (2012) 241-248, [arXiv:1112.4896].
- [59] R. Aaij *et al.* [LHCb Collaboration], *Measurement of b -hadron masses with exclusive $J/\psi X$ decays in 2010 data*, LHCb-CONF-2011-027.
- [60] R. Aaij *et al.* [LHCb Collaboration], *Measurement of the masses of the Ξ_b^- and Ω_b^-* , LHCb-CONF-2011-060.
- [61] R. Aaij *et al.* [LHCb Collaboration], *Search for the $X(4140)$ state in $B^+ \rightarrow J/\psi\phi K^+$ decays* Phys. Rev. **D85** (2012) 091103(R), [arXiv:1202.5087].
- [62] R. Aaij *et al.* [LHCb Collaboration], *Observation of $X(3872)$ production in pp collisions at $\sqrt{s}=7$ TeV*, Eur. Phys. J. C. **72** (2012) 1972. [arXiv:1112.5310].
- [63] LHCb Collaboration, *Letter of Intent for the LHCb Upgrade*, CERN-LHCC-2011-001.
- [64] LHCb Collaboration, *Framework TDR for the LHCb Upgrade*, LHCb-TDR-012.